Deletions at the SOX10 gene locus cause Waardenburg syndrome types 2 and 4.

Nadège Bondurand, Florence Dastot-Le Moal, Laure Stanchina, Nathalie Collot, Viviane Baral, Sandrine Marlin, Tania Attie-Bitach, Irina Giurgea, Laurent Skopinski, William Reardon, et al.

Deletions at the *SOX10* gene locus cause Waardenburg syndromes type 2 and 4.

Running title:

SOX10 deletions in WS2 and WS4

Nadege Bondurand[1,2,*], Florence Dastot-Le Moal[1,3], Laure Stanchina[1,2], Nathalie Collot[1,3], Viviane Baral[1,2], Sandrine Marlin[4], Tania Attie-Bitach[5], Irina Giurgea[1,2,3], Laurent Skopinski[3], William Reardon[6], Annick Toutain[7], Pierre Sarda[8], Anis Echaieb[9], Marilyn Lackmy-Port-Lis[10], Renaud Touraine[11], Jeanne Amiel[5], Michel Goossens[1,2,3] and Veronique Pingault[1,2,3]

[1] INSERM U841, IMRB, Département de génétique, Equipe 11, Créteil, F-94000, France.

[2] Université Paris 12, Faculté de Médecine, IFR10, Créteil, F-94000, France

[3] AP-HP, Groupe Henri Mondor-Albert Chenevier, Service de biochimie et génétique, Créteil, F-94000, France

[4] Service de Génétique, Centre de référence «Surdités génétiques», INSERM U587, Hôpital Armand Trousseau, APHP.

[5] INSERM U781, Université Paris5-Descartes, Faculté de Médecine, Service de Génétique Médicale, Hôpital Necker, AP-HP, Paris, France

[6] Our Lady's Hospital for Sick Children, Genetics, Dublin, Ireland

[7] Centre Hospitalo-Universitaire, Service de Génétique, Tours, France

[8] Centre Hospitalo-Universitaire, Service de Génétique, Montpellier, France

[9] Service de Chirurgie infantile, Hopital Pierre Zobda Quitman, CHU Fort de France, France

[10] Service de pédiatrie, Centre hospitalier universitaire de Pointe a Pitre, France

[11] CHU-Hôpital Nord, Service de Génétique, Saint Etienne, F-42000 France

*Address for correspondence and reprints : Nadège Bondurand. INSERM U841, IMRB, Département de génétique, Equipe 11, Hôpital Henri Mondor, 51 Avenue du Maréchal de Lattre de Tassigny, 94010, Creteil, France. email: nadege.bondurand@creteil.inserm.fr Tel: +33149812856. Fax: +33148993345

Abstract

Waardenburg syndrome (WS) is an auditory-pigmentary disorder that exhibits varying combinations of sensorineural hearing loss and abnormal pigmentation of the hair and skin. Depending on additional symptoms, WS is classified into four subtypes, WS1 to 4. Absence of additional features characterizes WS2. The association of facial dysmorphic features defines WS1 and 3 whereas the association with Hirschsprung disease (aganglionic megacolon) characterizes WS4, also called Waardenburg-Hirschsprung disease. Mutations within the genes encoding *MITF* and *SNAI2* have been identified in WS2, whereas mutations of *EDN3*, *EDNRB* and *SOX10* have been observed in WS4 patients. However, not all cases are explained at the molecular level, raising the possibility that other genes are involved or that some mutations within the known genes are not detected by commonly used genotyping methods. We used a combination of semi-quantitative fluorescent multiplex PCR (QMF-PCR) and Fluorescent in situ hybridization (FISH) to search for *SOX10* heterozygous deletions. We describe the first characterization of *SOX10* deletions in patients presenting with WS4. We also found *SOX10* deletions in WS2 cases, making *SOX10* a new gene of WS2. Interestingly, neurological phenotypes reminiscent of that observed in WS4 (PCWH syndrome) were observed in some WS2 patients with *SOX10* deletions. This study further characterizes the molecular complexity and the close relationship that links the different subtypes of Waardenburg syndrome.

Introduction

During development, the pluripotent neural crest cells migrate from the neural tube throughout the embryo along several pathways and give rise to different cell types, including glia and neurons of the peripheral nervous system, enteric neurons and glia, some of the craniofacial skeletal tissue and melanocytes of the skin and inner ear [1]. Defects in neural crest development are a significant cause of human disease. The term neurocristopathies collectively refers to these neural crest disorders, among which is Waardenburg syndrome (WS) [2-4]. The association of hearing loss and pigmentary abnormalities (heterochromia irides, white skin patches, white forelock…) characteristic of this syndrome results from an abnormal proliferation, survival, migration or differentiation of neural crest-derived melanocytes [3]. Several subtypes of WS were defined on the basis of the presence of additional symptoms.

Type I Waardenburg syndrome (WS1, MIM_193500) refers to the first cases described by Waardenburg [5]. Additional symptoms are dystopia canthorum and broad nasal root. Nearly all patients present with heterozygous *PAX3* mutations (PAX3, paired box gene 3, a member of the paired box family of transcription factor). Type III Waardenburg syndrome (WS3, MIM_148820) or Klein-Waardenburg syndrome, is an extreme presentation of type I with hypoplasia of limb muscles and is also due to heterozygous or homozygous mutations of *PAX3* [6; 7; 3].

Type II Waardenburg syndrome (WS2, MIM_193510) is characterized by deafness and pigmentation defects without additional features. Heterozygous mutations in the *MITF* gene (MITF, microphthalmia associated transcription factor, a basic-helix-loop-helix transcription factor) have been identified in about 15% of cases [8; 3]. Homozygous deletions of the *SNAI2* gene (Snail homolog 2, a C2H2-type zinc finger transcription factor) have also

been described in two patients [9]. Therefore, 85% of WS2 cases are still unexplained at the molecular level.

Type IV Waardenburg syndrome (WS4, MIM_277580), also called Shah-Waardenburg syndrome or Waardenburg-Hirschsprung disease, combines pigmentation defects, deafness and Hirschsprung disease [10]. Mutations in *EDNRB*, encoding the endothelin B receptor (a G-protein coupled transmembrane receptor), and *EDN3*, encoding its ligand endothelin-3, have been described. Homozygous (most frequently) or heterozygous mutations are found in WS4 probands, while heterozygous family members occasionally present with some of the features [11-14; 4; 15-17].

Dominant mutations of *SOX10* have also been identified in WS4 [18]. SOX10 is a key transcription factor of neural crest development. It is crucial for the survival and maintenance of pluripotency of migrating neural crest progenitors [19; 20], and also influences fate decisions and differentiation at later stages [21-25]. SOX10 belongs to the SOX family of transcription factors and is closely related to SOX8 and SOX9, the latter being involved in campomelic dysplasia [26; 27; 21; 23; 25]. All SOX proteins contain a DNA binding motif known as the high-mobility group (HMG) domain. In addition, SOX10, like SOX8 and SOX9, contains a transactivation domain located in the C-terminal part of the protein and a dimerization domain immediately preceding the HMG domain [21; 28; 29; 22]. Functional studies revealed the importance of these domains for monomeric or dimeric DNA binding and transactivation of natural target genes [21; 22]. Among them are genes/factors crucial for the specification and differentiation of melanocytes or enteric nervous system development, such as *MITF/Mitf*, *TRYP2/Dct* (Dopachrome tautomerase), tyrosinase, *EDNRB*, and the *RET* protooncogene [30-41]. SOX10 targets also include genes important for glia development and identity such as *MPZ* (Myelin protein zero, P0), *MBP* (Myelin basic protein), and *GJB1* (encoding the gap junction protein connexin 32) [29; 42-46].

The *SOX10* mutations characterized so far are mostly truncating mutations: nonsense or frameshift and one splice mutation, which most often remove all or part of the transactivation domain [18; 47-58]. An insertion of two amino acids and an amino acid substitution in the HMG domain, as well as two mutations of the stop codon supposed to give rise to elongated SOX10 protein, have also been described [18; 48; 49; 53]. Unexpectedly, some of the patients with *SOX10* mutations present with chronic intestinal pseudo-obstruction instead of Hirschsprung disease [51; 55], and/or neurological features, either peripheral demyelinating neuropathy or central neuropathy, or both, leading to a syndrome called PCWH (Peripheral demyelinating neuropathy-Central dysmyelinating leukodystrophy-Waardenburg syndrome-Hirschsprung disease) [57]. This more severe disease is mostly due to mutations in the last coding exon of *SOX10* and has been proposed to occur when the mutant mRNAs escape the non-sense RNA decay (NMD) pathway [57].

However, some WS4 cases remain unexplained at the molecular level, suggesting that other genes may be involved, or that some mutations within the known genes are not detected by the methods commonly used for genotyping. Therefore, we used semi-quantitative fluorescent multiplex PCR (QMF-PCR) to search for heterozygous *SOX10* deletions. Here we describe the first characterization of *SOX10* deletions in patients presenting with WS4. In light of the phenotypic variability observed among patients with *SOX10* point mutations, we also searched for *SOX10* deletions in unexplained cases of WS2 and found several, making *SOX10* a new gene of WS2.

Subjects and methods

Subjects

We investigated a total of 30 patients presenting with the classic form of WS4 or PCWH: 29 of them negative for *EDN3, EDNRB* and *SOX10* point mutations, and one found hemizygote for a *SOX10* point variation within the course of this work. Our study also included 30 WS2 patients without *MITF* mutations. Clinical information and DNA samples were obtained with informed consent according to French law for genetic testing. The main clinical findings in patients presenting with *SOX10* gene deletions are summarized in Table 4. Detailed clinical descriptions of the patients presenting with *SOX10* gene deletions are as follows:

Patient 1, a one-year-old male, was born at term of unrelated parents after unremarkable pregnancy and delivery. At 48 hours of life he presented with clinical signs of meconium plug syndrome due to a short-segment Hirschsprung disease. Bilateral absence of responses to brainstem auditory-evoked potential strongly suggested bilateral deafness. He also had hair and skin hypopigmentation and bilateral cryptorchidism.

Patient 2, a 13-year-old male, was born at term of unrelated parents, following a pregnancy complicated by gestational diabetes. He has two healthy sisters. He had delayed psychomotor development, hair and skin hypopigmentation, sapphire blue eyes and short-segment Hirschsprung disease operated at the age of 15 months. Nine months later, he had implementation of a unilateral cochlear device for profound bilateral congenital deafness. In spite of good perceptual results, he had speech and sign language impairment because of dyspraxia. He had mild mental retardation, anosmia, hypermetropia and dental enamel abnormalities.

Patient 3 is a 36 year-old male, born at term of unrelated parents after unremarkable pregnancy and delivery. In the neonatal period, he had axial hypotonia and delayed psychomotor development: he could hold his head up at 1 year, sit alone at 3 years and walk

at 4-5 years. He had hair and skin hypopigmentation, sapphire blue eyes, short-segment Hirschsprung disease and profound bilateral congenital deafness for which he had implementation of a unilateral cochlear device at the age of 32 years. Temporal bone CT scan revealed a bilateral vestibular malformation and hypoplasia of the external and posterior semicircular canals. He also presented anosmia, bilateral cryptorchidism and hypogonadotropic, hypogonadism, bone-age and pubertal growth delay. He now has mild mental retardation with marked abstraction difficulties.

Patient 4, a 9-year-old male, was born at term of unrelated parents after unremarkable pregnancy and delivery. He began to walk at 21 months of age. A bilateral sensorineural hearing impairment was discovered at 6 months of age and progressed to profound deafness. A cochlear implantation was performed with success in terms of understanding and of language. Temporal bone CT scan revealed a symmetrical bilateral vestibular malformation with dilatation of the vestibule, hypoplasia and dilatation of the external and posterior semicircular canals. He presented skin, irides and retina hypopigmentation. He had no history of constipation and his neurological development was normal. His brother presented with similar clinical symptoms. No other cases of hearing defect or pigmentation anomalies were observed in the family.

Patient 5 a 8-year-old male, was born at term of unrelated parents after unremarkable pregnancy and delivery. He began to walk at 20 months of age. A profound bilateral sensorineural hearing impairment was diagnosed at 5 months of age. Temporal bone CT scan did not reveal any malformation of the inner ears. He presented with skin depigmentation and hypoplastic irides. He had no history of constipation and his neurological development was normal. His mother presented a bilateral severe sensorineural prelingual hearing impairment. She was born with a frontal white forelock and a heterochromia (one green iris, one hypoplastic).

Patient 6, now aged 8, is the third child of a non-consanguineous couple from the French Caribbean Islands. At 9 months of age, a severe bilateral sensorineural hearing impairment was diagnosed, and progressed to a bilateral profound deafness by 8 years of age. He presented a white frontal forelock at birth and heterochromia irides (one black and one hypoplastic) but has no skin depigmentation. He began walking at 17 months of age and has no history of severe constipation or neurological anomaly.

Patient 7, now aged 23, was born at term of unrelated parents after unremarkable pregnancy and delivery. He presented with a white frontal forelock (now disappeared), skin hypopigmentation, sapphire blue eyes, pectus excavatum and statural growth following the 3rd percentile. He has no constipation problems. In addition this patient has severe autism and developmental delay (he started to walk at 3 years, is not toilet-trained and has little autonomy). Brain CT scan was normal. Bilateral sensorineural deafness was diagnosed at the age of 9 months and he had cochlear implementation up to the age of 13 years. However, due to severe behavioral problems, hearing loss has not been evaluated since.

Patient 8 was born at term of unrelated parents after unremarkable pregnancy and delivery. She presented with severe congenital heart disease associating double outlet right ventricle, transposition of the great arteries, pulmonary atresia, patent ductus arteriosus, ventricular septal defect and atrial septal defect. A white forelock and a duplication of the thumb on the left side were noted. At age10 months, she presented obvious evidence of deafness, medial flare of the eyebrows, strabismus and general hypotonia. Brain MRI scan at age 14 months showed delayed myelination. Specific evaluation of the skin on Wood's lamp revealed multiple hypopigmented areas. She had no history of constipation. Heart surgery had been partially successful but episodes of unexplained bradychardia and peripheral cyanosis were observed and the patient died at the age of 19 months.

Semi quantitative fluorescent multiplex PCR (QMF-PCR)

QMF-PCR has been shown to be a sensitive method for the detection of gene dosage anomalies, and has been successfully used in our laboratory to characterize deletions and duplications within several genes [59; 60]. We adapted the protocol previously described [61; 59] to screen for *SOX10* gene deletions. Briefly, the 3 coding exons of the *SOX10* gene, exon 4 of *POLR2F* and 4 regions located 5' of *SOX10* were amplified in two multiplex reactions. The beginning of exon 3 and the middle of the exon 5 coding sequences are not covered by the amplicons, however a deletion restricted to one of these region would have been found during the point mutation screening. Non-coding regions of *SOX10* were not studied. GenBank accession number, position, sequences of the primers, and PCR product sizes are shown in Table 1. In each set, two controls were used: *DSCR1* located on chromosome 21 and *F9* located on chromosome X (see reference genes in Table 1). The reverse primers were labelled with the fluorescent phosphoramidite 6-FAM dye. Amplifications were performed in duplicates in 25µl reactions using the QIAGEN Multiplex PCR kit (Qiagen, France), with 75 ng of genomic DNA, a mix of primers (concentration range 0.1 to 1 µM), and 5% DMSO. The reaction started with an initial denaturation of 15 min at 95°C followed by 22 cycles at 95°C for 30 sec, 55°C (multiplex reaction mix 1) or 58°C (multiplex reaction mix 2) for 30 sec, and 72°C for 45 sec with an increment of 3 sec per cycle, and a final extension of 10 min at 72°C. Then, 3µl of the purified PCR products were processed as previously described [59]. Two control DNAs (male and female) were included in each experiment. Results were analysed by superimposing fluorescent profiles of tested patients and controls and by calculating dosage quotient (DQ) [59]. DQ values below 0.6 were considered as potential deletions. Table 2 summarizes examples of DQ values obtained.

Molecular characterization of rearrangements

When QMF-PCR revealed a short size deletion (only one exon removed), the genomic region encompassing the deletion breakpoint was amplified either by classic or long range PCR

using Dynazyme Ext DNA polymerase (Ozyme, France) or the Expand Long Template PCR system (Roche Diagnosis, France), respectively. The resulting PCR fragments were cloned into the TOPO-TA cloning kit Dual promoter or the TOPO-XL PCR cloning kit (Invitrogen, France) and sequenced. Bioinformatic analysis was performed to predict the functional consequences of intragenic deletions using Netgene2 (neural network predictions of splice sites in human) and HMMgene (gene prediction structure) softwares.

In the case of whole *SOX10* gene deletions, fluorescent in situ hybridization (FISH) was used to confirm the QMF-PCR results. Molecular cytogenetic studies were performed on chromosomes prepared from cultured fibroblasts (patient 8) or peripheral blood cells. Metaphase chromosomes were obtained according to standard techniques. FISH was performed as previously described [62]. PAC and BAC clones used in FISH experiments were provided by the BACPAC Resources Center, (CHILDREN'S HOSPITAL OAKLAND, Oakland, USA) or by The Wellcome Trust Sanger Institute (Cambridge, UK). Clones localized on chromosome 22q12-q13.2 (CTA-415G2, LL22NCO1-95B1, RP1-288L1, CTA-714B7, RP1-41P2, CTA-390B3, RP5-1177I5, RP1-37E16, RP3-466N1, RP5-1014D13, RP5-1039K5, CTA-228A9, CTA-447C4, RP1-5O6, RP3-434P1, RP1-319F24, RP3-508I1S, RP3-327516, CTA-150C2, RP4, 742C19, LL22NC03-10C3) were directly labelled with Cy3. The control probes (RP1-41P2 and RP1127L4) were directly labelled with FITC, and chromosomes were counterstained with Dapi. The specific signal intensity and its sublocalization along the chromosome axis were analysed using a Leica fluorescence microscope equipped with the Visilog-6 program (Noesis, Les Ulis, France). Based on FISH results, additional QMF-PCR primers were designed to delineate the extent of deletions. Position and sequences of these additional primers are reported in Table 3.

Chromosome segregation analysis

Seven chromosome 22 microsatellites (D22S420; D22S539; D22S315; D22S280; D22S283; D22S423; D22S274) were analysed in patient 3 and his parents using the linkage mapping set (Applied Biosystem, USA) according to the manufacturer's instructions.

***SOX10* point mutation screening in WS2 patients**

In the absence of a full description of the 5'UTR non-coding exon(s) of *SOX10*, we conserved for convenience the exon numbering system previously used, i.e. non-coding exons 1 and 2, ATG codon in exon 3 and stop codon in exon 5 [18]. Three sets of primers were used to amplify the *SOX10* gene fragments covering coding exons 3 to 5 and intron-exons boundaries (First set: exon 3, 5'-ACCCACCTAGAGTCTGGCATG-3' and 5'-CTCGGCTACCCTGAATCCAC-3', size of PCR product 733 bp; second set: exon 4, 5'-CCACAAATCATAGGGCACAG-3' and 5'-TAGAGTCCAGGGTCTCATTG-3', size of PCR product 523 bp; third set: exon 5, 5'-CCTGCCTCTAACCTGCTTCC-3' and 5'-ACCTCCTTCTCCTCTGTCCA-3', size of PCR product 997 bp). The PCR covering the exon 3 region contained 10% DMSO. Resulting PCR products were sequenced using a 16 capillary ABI Prism sequencer and the Terminator Cycle Sequencing kit. Additional internal sequencing primers were used for exon 3: 5'- GCGAGCTGGGCAAGGTCAAG-3' and 5'-TCGCCGTCCTGCTGCTCCTT-3' and exon 5: 5'-GGATGCCAAAGCCCAGGTGA-3' and 5'-GTAGGCGATCTGTGAGGTGG-3'.

Plasmids, cell culture, transfection and reporter assays

The pECE-SOX10, pECE-SOX10-E189X, pECE-SOX10-Y313X, pECE-SOX10-482ins6, pECE-PAX3, pECE-EGR2, pGL3-MITFdel1718, pGL3-Cx32 vectors were previously described [30; 43]. The p.Val92Leu mutation (named V92L for convenience) was introduced within the pECE-SOX10 construct by site directed mutagenesis using the Quick change mutagenesis kit (Stratagene, Netherlands). Luciferase assays and immunofluorescence were

performed 24h after transfection of HeLa cells as previously described [30; 43; 63]. The SOX10 antibody used for immunofluorescence was previously described [64]. The P0 construct was kindly provided by M. Wegner [29].

Results

Identification of *SOX10* deletions in patients presenting with WS4 or PCWH

In our experience, about 20-40% of affected individuals with the WS4 or PCWH phenotypes have no mutations within *SOX10*, *EDN3* or *EDNRB* genes identifiable by conventional genetic analysis using DNA sequencing of PCR-amplified gene segments. As this technique does not detect heterozygous deletions, we decided to search for *SOX10* deletions or rearrangements by semi-quantitative fluorescent multiplex PCR (QMF-PCR). Our study included 29 patients presenting with the classic form of WS4 or PCWH previously found negative for *SOX10*, *EDN3* and *EDNRB* point mutations. We first analyzed the 3 coding exons of *SOX10*, part of the *POLR2F* downstream gene, and sequences located up to 50 kb upstream of *SOX10* (S1 to S4, see Fig.1A). One of them, S1, was previously described as a *SOX10* enhancer [65] (see Table 1 for sequences of primers named P1 to P9).

We identified two heterozygous deletions (Patients 1 and 2; see case reports and Table 4 for clinical descriptions). The first, found in a patient presenting with a classical WS4 phenotype, removes part of exon 5 (Fig.1A, patient 1). PCR amplification using primers located in intron 4 and exon 5, cloning and sequencing of the resulting products revealed a complex rearrangement combining a 1128 bp deletion encompassing 740 bp of the fourth intron and 388 bp of exon 5, and a 3 bp insertion (Fig.1B). The other deletion, found in a PCWH patient, includes the whole *SOX10* gene, *POLR2F* and the upstream S4 sequence (Fig.1A, patient 2). FISH analysis using a BAC encompassing the whole region (clone RP5-1039K5, Fig.1A) confirmed the QMF-PCR results. Indeed, we observed a significantly decreased signal on one of the chromosomes 22 in all the metaphases (Fig 1C, patient 2), showing that the deletion only removes part of the RP5-1039K5 probe (S1 to S3 are not deleted, see Fig.1A). In each of the 2 cases, the analysis of parents DNA by QMF-PCR revealed the de novo occurrence of the deletion (Table 4).

Detection of a *SOX10* deletion in a PCWH patient with p.Val92Leu variation

Sequencing of the *SOX10* coding exons and intron-exon boundaries in newly recruited patients led us to identify a new point mutation (nucleotide substitution c. 274G>C in exon 3) that predicts the replacement of a Valine by a Leucine at codon 92 (p.Val92Leu) in a patient presenting with PCWH (patient 3; see case report and Table 4 for clinical description). This amino acid substitution affects a residue located within a region directly preceding the HMG domain that is not only well conserved between SOX10 proteins across evolution, but also with the SOX E members, SOX8 and 9 (Fig.2A) [28]. Surprisingly, this variation was observed at the homozygous state, and therefore contrasts with the heterozygous state of all the mutations identified to date. The parents were not consanguineous nor presented any feature of the disease, except for early greying in the mother. We found the mutation at the heterozygous state in the father's DNA only. The analysis of seven chromosome 22 microsatellites excluded a chromosome segregation abnormality and the possibility of a chromosome 22 paternal isodisomy (data not shown).

To explain these data, we searched for a deletion or rearrangement of *SOX10* that would result in a hemizygous p.Val92Leu mutation. QMF-PCR experiments indeed unravelled a deletion that removes the whole *SOX10* gene, along with the upstream and downstream sequences tested (Fig.1A, patient 3). FISH analysis using the BAC clone RP5-1039K5 confirmed the presence of a deletion encompassing the whole region (Fig.1C, patient 3, presence of only one signal on the normal chromosome 22). Analysis of parents' samples established the de novo occurrence of the deletion (Table 4).

These results suggested that the phenotype of patient 3 is related to this large deletion, but we could not exclude that the p.Val92Leu variation contributes to the phenotype. To test this possibility, we introduced the mutation into the *SOX10* cDNA and analysed its functional consequences *in vitro.* Immunofluorescence experiments on HeLa cells transiently

transfected with wild type or p.Val92Leu constructs revealed correct nuclear localization of the mutant protein (Fig.2B).

The region affected by the mutation was previously implicated in DNA dependent dimerization, both in SOX10 and SOX9 [29; 42; 45; 66]. Moreover, a SOX9 mutation located in the same region (p.Ala76Glu) was shown to selectively abrogate DNA-dependent dimerization and thus interfere with promoter activation via natural target sites that require binding of SOX9 as dimers [66]. We therefore analysed the transactivation potential of the p.Val92Leu mutant on two promoters previously shown to contain monomeric or dimeric SOX10 binding sites, respectively MITF and Cx32. Indeed, SOX10, in synergy with PAX3, regulates *MITF* expression by directly binding to its promoter as monomers [30; 33]. SOX10, on the other hand, regulates *GJB1* (encoding connexin 32, Cx32) expression by directly binding to its promoter on a dimeric configuration and in synergy with its cofactor EGR2 [43; 67] (insets in Fig.2C and D). Cotransfection of either promoter with wild type or p.Val92Leu SOX10 mutant, and/or SOX10 cofactors (PAX3 and EGR2), revealed that normal and mutant SOX10 have similar transactivation capacities on these promoters, alone or in synergy with the cofactors (Fig.2C and D). In contrast, three previously identified SOX10 mutations (p.Glu189X, c.482ins6, and p.Tyr313X, respectively named E189X, 482ins6 and Y313X in fig 2C and D) failed to transactivate these reporter constructs, as previously described [30; 43; 68]. We also performed similar experiments using another SOX10-responsive promoter known to contain SOX10 dimeric binding sites, P0, and found no difference between wild type and p.Val92Leu mutant transactivation capacities (data not shown). Therefore, the p.Val92Leu variation does not seem to affect SOX10 function, at least in vitro, arguing in favour of the deletion as the cause of the phenotype observed in this patient.

Molecular characterization of large deletions in PCWH patients

To define the boundaries of the deletions encompassing the *SOX10* gene found in patients 2 and 3, we extended our analysis to adjacent regions using two complementary strategies: FISH and QMF-PCR.

In case of patient 2, we chose additional sets of QMF-PCR primers localised between upstream S3 and S4 sequences, allowing us to map the telomeric border of the deletion to a region located 24 to 31 kb upstream of the *SOX10* start codon (Fig.3B, patient 2). In parallel, FISH experiments with the probe RP5-1014D13 (covering regions proximal to *POLR2F*, including *MICAL-L1* gene, see Fig.3), showed a distinct signal on both chromosomes 22, positioning the centromeric border of the deletion between *POLR2F* and *MICAL-L1* genes (Fig.3A). We chose additional sets of QMF-PCR primers within the genes located in the region and localized the end of the deletion between exons 3 and 4 of the *C22ORF23* sequence (Fig.3B and Table 3 for corresponding primers). The whole deletion therefore encompasses 56 to 68 kb including, in addition to *SOX10*, *POLR2F* and part of *C22ORF23* genes.

In the case of patient 3, we carried out FISH analysis using RP5-1014D13 on one side, and CTA-228A9 on the other. This allowed us to localize the centromeric border of the deletion between RP5-1014D13 (that shows hybridization on both chromosomes 22) and RP5-1039K5 (that shows only one signal on normal chromosome 22) (Fig.3A and Fig.1C). The telomeric border was localized within the CTA-228A9 (we observed a significantly decreased signal on one of the chromosomes 22 in all the metaphases, Fig.3A). Based on these results, we repeated a series of multiplex PCR using primers located within *C22ORF23* or *MICAL-L1* genes on one side and in the *PLA2G6* gene on the other, and could finally determine the deletion boundaries between intron 9 and exon 8 of the *MICAL-L1* gene and between exon 4 and intron 2 of the *PLA2G6* gene (Fig.3B and Table 3 for corresponding primers). The whole deletion therefore encompasses 213 to 222 kb, including part of *MICAL-*

L1 gene, *C22ORF23*, *POLR2F, SOX10, PICK1, SLC16A8, BAIAP2L2* genes, and part of the *PLA2G6* gene.

Identification of *SOX10* deletions in WS2 patients

WS4 patients with *SOX10* point mutations or deletions exhibit a large variability and an incomplete penetrance of each feature (ie, fully blue irides, patchy blue irides or normal eyes; large, small or none depigmented skin patches; short or long segment Hirschsprung disease or chronic intestinal pseudo-obstruction…). Interestingly, we previously described a c.1076delGA mutation in a patient with a classical form of WS4 [18], that was inherited from a mother presenting with deafness and white forelock only. We also described a p.Ser135Thr (S135T) mutation in a patient presenting with a peculiar phenotype named "Yemenite deaf-blind hypopigmentation syndrome" without any intestinal dysfunction [48]. These two phenotypes, which are reminiscent of that observed in WS2 patients, prompted us to search for *SOX10* deletions in unexplained cases of WS2. Screening of 30 cases (previously found negative for *MITF*) by means of QMF-PCR allowed us to identify 5 different *SOX10* deletions (patients 4 to 8; see case report and Table 4 for clinical descriptions).

The first encompasses exon 3 (Fig.4A, patient 4). PCR amplification using sets of primers located in exon 3 and intron 3, followed by cloning and sequencing of the PCR products revealed a 253 bp deletion removing 210 bp of exon 3 and 43 bp of intron 3 (Fig.4B). Interestingly, the patient's brother, who presented similar WS2 features, also carries the deletion (Fig.4B). However, it was not found in the parent's DNA, suggesting germline mosaicism. We analysed hair roots, buccal and uroepithelial cell samples of both parents by PCR amplification, and found the band specific to the deleted allele in the mother's uroepithelial cell sample, showing the existence of somatic mosaicism (Fig.4C and Table 4).

The second deletion encompasses 1777 bp and removes the whole exon 4, 1112 bp of intron 3 and 396 bp of intron 4 (Fig.4A and D, patient 5). The father's DNA was not available.

However analysis of the mother's DNA by QMF-PCR and PCR sequencing techniques revealed the deletion is maternally inherited, in agreement with the observation that the mother also presents with WS2 (Fig.4D and Table 4).

The other three deletions included the whole *SOX10* gene, as well as *POLR2F* and the upstream S4 sequence (Fig.4A, patients 6, 7 and 8). Additionally, sequences S1 to S3 were deleted in patients 7 and 8. FISH analysis using the BAC clone RP5-1039K5 confirmed the presence of a deletion encompassing the whole region analysed in patient 8 (Fig.4A and E). Analysis of parents' samples revealed the de novo occurrence of the deletions in these three patients (Table 4).

Molecular characterization of large deletions in patients presenting with WS2

To define the boundaries of the 3 deletions encompassing the whole *SOX10* gene we extended our analyses to adjacent regions. In the absence of material to perform FISH experiments in patients 6 and 7, we determined the boundaries of the deletion by repeating many sets of multiplex QMF-PCR (Fig.5B and data not shown). In the case of patient 6, additional sets of QMF-PCR primers between upstream S3 and S4 sequences allowed us to map the telomeric border of the deletion to a region located 20 to 21 kb upstream to the *SOX10* start codon. The centromeric border was localized between genes *CACNG2* and *MYH9*, therefore delimitating a deletion of 1.3 to 1.6 Mb that removes at least 42 genes including *SOX10* and *TRIOBP* (Fig.5B).

Patient 7's deletion removes 574 to 898 kb. Indeed, boundaries were located between *LGALS2* and *SH3BP* on one side and *C22ORF5* and *KDELR3* on the other side. The deletion therefore encompasses 23 genes among which *SOX10*, *TRIOBP* and *PLA2G6* (Fig.5B).

In the case of patient 8, FISH analysis was performed using several probes including CTA-415G2, LL22NC01-95B1, RP1-288L1, CTA-714B7, RP5-1177I5, RP1-37E16, CTA-228A9, RP1-5O6, RP3-434P1, CTA-150C2, RP4-742C19. The telomeric border was localized within

the RP4-742C19 BAC (we observed a significantly decreased signal on one of the chromosomes 22 in all the metaphases, Fig.5A) and the last centromeric deleted BACs was LL22NCO1-95B1 (Fig.5B and data not shown). QMF- PCR using primers within some of the genes located in the region confirmed the results, therefore delimiting a deletion of 5.5 to 6.1 Mb encompassing 102 different genes including *SOX10*, *LARGE , RASD2, RBM9, MYH9, CACNG2, TRIOBP*, *PLA2G6*, *KCNJ4*, and *NPTXR* (Fig.5B and data not shown).

The identification of five *SOX10* deletions in 30 cases studied revealed that *SOX10* is a new gene of WS2, and thus prompted us to screen for *SOX10* point mutations. However, we failed to detect any mutation by DNA sequencing of the three *SOX10* coding exons. Taken together, these results make *SOX10* the third gene involved in WS2 with an estimated frequency (15%) similar to that of *MITF*.

Discussion

Considering our panel of patients presenting with WS4 (classic forms of WS4 and PCWH), we estimated that for 20-30 % of them the phenotype is due to *EDN3* or *EDNRB* point mutations, and for 40-50 % to *SOX10* point mutations. In WS2 patients, mutations in the *MITF* gene were identified in about 15% of cases. Thus, 20-40% of WS4 and 85% of WS2 cases remained unexplained at the molecular level, raising the possibility that other genes are involved, or that some mutations within the known genes are not detected by the methods commonly used for genotyping. In this study, we describe the first characterization of *SOX10* deletions in patients presenting with WS4 and WS2. We found 3 deletions among 30 WS4 cases. Taking into account the fact that we only tested DNAs of patients negative for *SOX10*/*EDN3*/*EDNRB* point mutations, we estimate that *SOX10* deletions are involved in about 5 % of all WS4 patients. We also found 5 deletions among 30 WS2 cases. As we only tested patients negative for *MITF* mutations, we can estimate that *SOX10* deletions accounts for approximately 15% of all WS2 cases. These results extend the spectrum of *SOX10* mutations found in WS4 patients, and make *SOX10* the third gene involved in WS2 with an estimated frequency similar to that of *MITF*. In terms of molecular diagnosis, *SOX10* deletions should now be searched for when no *SOX10* point mutations (PCWH), or no *SOX10*, *EDN3* and *EDNRB* point mutations (classical form of WS4), are found. More importantly, *SOX10* deletions should be considered as a first step analysis in WS2, as well as *MITF* mutations.

Full characterization of the 8 deletions by PCR and sequencing, or a combination of QMF-PCR and fluorescent in situ hybridization (FISH), revealed 8 different deletion events ranging from the deletion of a single exon of *SOX10* to that of up to 6 Mb around the *SOX10* locus (Table 4). Both intragenic and full *SOX10* deletions were observed either in WS2 or WS4. Intragenic deletions involved different exons. The observation of sequences surrounding the

breakpoints of the 3 intragenic deletions revealed no clear mechanism except for patient 5, where the deletion occurred between two hexanucleotide repeats 'tggtgg', retaining one copy. Bioinformatic analysis using the Netgene2 and HMMgene software was performed to predict the functional consequences of these deletions. In case of patient 1, the rearrangement was predicted to activate a cryptic splice acceptor site within exon 5, located downstream the stop codon (780 nucleotides after the usual acceptor site, estimate frequency of 97%). The predicted protein would lack the last 206 amino acids, replaced by 27 unrelated amino acids, thereby removing the transactivation domain. In case of patient 4, the deletion removed the exon 3-intron 3 boundary. In silico analysis revealed that this deletion could result in translation of a short intronic sequence with a nearly immediate stop codon (5 amino acids downstream), the resulting protein being devoid of all functional domains. Alternatively, the use of a cryptic splice donor site (estimated frequency 55% or 88% depending on the program used), located 55 nucleotides downstream the missing donor site, could produce a protein lacking 69 amino acids, removing the dimerization domain and half of the HMG domain but leaving the transactivation domain intact. In case of patient 5, the Netgene2 software predicted that the deletion could lead to exon 4 skipping, therefore resulting in a frameshift and a truncated protein of 189 amino acids with 47 unrelated amino acids in the carboxyterminal part. Half of the HMG domain and the following domains would be removed. Unfortunately, there is no SOX10-expressing tissue easily accessible by non invasive methods in patients, precluding analysis of the protein produced in vivo.

Most of the *SOX10* disease-associated point mutations identified so far, regardless of whether they cause WS4 or PCWH, result in premature termination codons (PTCs). An explanation for the presence or absence of a neurological phenotype (ie, central or peripheral) that characterizes the PCWH syndrome has been hypothesized to be related to non-sense mRNA decay (NMD) process [57]. Truncating mutations located in the first coding exons (exons 3 and

4) activate the NMD RNA surveillance pathway, leading to haploinsufficiency and classic forms of WS4. On the other hand, truncating mutations located in the last coding exon (exon 5) escape non-sense mRNA decay, leading to translation of an abnormal SOX10 protein with a dominant negative effect, therefore resulting in the more severe PCWH phenotype. Considering the published *SOX10* point mutations [18; 47; 49; 50; 52-58] and our unpublished cases, we observed that the length of intestinal aganglionosis may also fit the NMD hypothesis, as all the point mutations associated with the long segment HSCR are located in the fifth exon. Accordingly, full deletions of *SOX10* would be expected to cause classic forms of WS4 with short segment HSCR as a result of haploinsufficiency. All three patients indeed present with a short form, however two of them have a mild PCWH syndrome, an observation that does not match the non-sense mRNA decay hypothesis (Table 4).

We wondered whether the PCWH syndrome may also result from other mechanisms, at least in some of the patients. Interestingly, one of the PCWH patients with a *SOX10* deletion (patient 3) also carries a SOX10 valine to leucine substitution at the hemizygous state. This variation, which could worsen the phenotype of the patient, is located in a highly conserved region crucial to mediate DNA-dependent dimerization. We thus reasoned that the p.Val92Leu variation, although not a drastic substitution, might interfere with the formation of SOX10 dimers and thus specifically hamper promoter activation via natural target sites that require binding of SOX10 dimers. We therefore compared wild type and p.Val92Leu SOX10 transactivation capacities on *MITF* and *GJB1* (Cx32) promoters, containing monomeric or dimeric binding sites, respectively, and found no differences. These results suggest that the p.Val92Leu variation does not affect SOX10 function at least in vitro, arguing in favor of the deletion as the major or sole cause of the PCWH phenotype observed.

A contiguous gene syndrome may also account for the neurological features. The deletion identified in patient 3 encompasses the *PLA2G6* gene known to be involved in a recessive

neurological defect (infantile neuroaxonal dystrophy 1, INAD1; neurodegeneration with brain iron accumulation; Karak syndrome) [69]. However, this gene is not deleted in patient 2 who has a mild PCWH syndrome resembling that of patient 3, suggesting that the heterozygous *PLA2G6* deletion is not involved in the phenotypic expression of the disease.

In WS2 as in WS4, the largest deletions are found in patients presenting with additional symptoms, suggesting that some features may be influenced by the presence of other genes. Indeed, several genes removed by one or more of the deletions have a well-established neurological role (*LARGE, RASD2*, *RBM9*, *CACNG2*, *KCNJ4*, *NPTXR*). Two genes involved in human hearing loss are also located within some of the deleted regions: *TRIOBP* (recessive non-syndromic deafness DFNB28 [70]) and *MYH9* (Epstein and Fechtner syndromes, dominant progressive isolated deafness DFNA17 [71; 72]). However, when comparing all 8 patients, we observed no clear correlation between the deletion of one of these genes, and the presence of neurological features or the deafness phenotype. In fact, as for *SOX10* point mutations, *SOX10* deletions by themselves might be sufficient to explain the phenotypes observed. On the other hand, the autism of patient 7, and the cardiac defects of patient 8, have not previously been linked to *SOX10* mutations and may result from the deletion of additional genes. We found no evidence of a known gene removed by patient 8's deletion, which could explain the cardiopathy, but this deletion encompasses 102 genes and they are not all functionally characterized. In autism, recurrent deletions of chromosome 22q13 have been characterized [73], including a frequent breakpoint within the *SHANK3* gene [74]. However, this region is distal to the deletion found in patient 7. The question as to whether the association with autism in patient 7 is fortuitous or results from the deletion remains open.

The Waardenburg syndrome subtypes were initially clinically defined. It appears however that this classification does not reflect the molecular mechanisms. Indeed, an overlap between WS1 and WS3 has already been reported, and we now report an overlap between WS2 and

WS4. In developmental syndromes, incomplete penetrance of some features is commonly observed. Incomplete penetrance of Hirschsprung disease is described both in isolated and in syndromic forms of the disease and it may result from different mechanisms, including genetic modifiers [75; 76]. In the case of Waardenburg syndrome, incomplete penetrance of Hirschsprung disease could explain the overlap between WS2 and WS4. However, with regard to this hypothesis, it is surprising not to find *SOX10* point mutations in WS2. To our knowledge, no genetic disorder has been described to result exclusively from deletions of the causative gene. It is possible that the penetrance of one feature varies between deletions and truncating point mutations, as shown for example in Von Hippel-Lindau disease [77]. In our case, incomplete phenotypic penetrance may be explained by tissue-specific compensation of the loss of SOX10 by other SOX proteins having partly redundant function, such as SOX8 and SOX9. Interestingly, in mice that expressed SOX8 instead of SOX10, the enteric defect was partially or totally rescued in homozygotes or heterozygotes, respectively, while the pigmentation defect was not [78]. As a result, SOX10 haploinsufficiency may be compensated by SOX8/9 during enteric nervous system development, explaining the low penetrance of Hirschsprung disease associated to *SOX10* deletions (leading to WS2 or WS4). In contrast, the presence of a truncated SOX10 protein may impair SOX8/9 function, resulting in a fully penetrant enteric phenotype (leading to WS4 only). However, it is possible that screening larger numbers of WS2 patients will result in the identification of *SOX10* point mutations. An increasing diversity of clinical features is reported in Waardenburg syndrome: some WS4 patients present with pseudoobstruction instead of Hirschsprung disease, and other with myelination defects of the peripheral and central nervous system, i.e. PCWH syndrome. In this study, patients 7 and 8 presented with WS2 and central and peripheral neurological features typical of PCWH – formally a new syndrome, indicating a continuum from isolated WS2 to severe PCWH. Based on our observation of *SOX10* deletions in WS2, it appears

possible that *EDN3* and *EDNRB* mutations also play a role in WS2. Indeed, in a subset of WS4 families with *EDN3* or *EDNRB* point mutations, heterozygous relatives present with a diversity of features that may occasionally recalls WS2. It therefore appears necessary to undertake a more complete molecular analysis (point mutations, but also deletions) of all the genes involved in WS2 or WS4 (*MITF*, *EDN3*, *EDNRB*). These comprehensive studies are necessary to fully document the molecular complexity and close relationship that link the different subtypes of Waardenburg syndrome, and to reappraise their current clinical classification.

Acknowledgments

This work was supported by INSERM and Agence Nationale de la Recherche (ANR-05-MRAR-008-01).

Web Resources

Accession numbers and URLs for data presented herein are as follows:

CHILDREN'S HOSPITAL OAKLAND, Oakland, USA, http://bacpac.chori.org/

Wellcome Trust Sanger Institute Cambridge, UK, http://www.sanger.ac.uk/

GenBank, http://www.ncbi.nlm.nih.gov/GenBank/,

Online Mendelian Inheritance in Man (OMIM), http://www.ncbi.nlm.nih.gov/Omim

Netgene2, neural network predictions of splice sites in human,

http://www.cbs.dtu.dk/services/NetGene2/

HMMgene, gene prediction structure, http://www.cbs.dtu.dk/services/HMMgene/.

References

1. Le Douarin NM, and Kalcheim C (1999) The neural crest. Cambridge University press

2. Bolande RP (1974) The neurocristopathies: a unifying concept of disease arising in neural crest maldevelopment. Hum Pathol 5:409-429

3. Read AP, Newton VE (1997) Waardenburg syndrome. J Med Genet 34:656-65

4. Amiel J, Lyonnet S (2001) Hirschsprung disease, associated syndromes, and genetics: a review. J Med Genet 38:729-39

5. Waardenburg PJ (1951) A new syndrome combining developmental anomalies of the eyelids, eyebrows and nose root with pigmentary defects of the iris and head hair and with congenital deafness. Am J Hum Genet 3:195-253

6. Baldwin CT, Hoth CF, Amos JA, da-Silva EO, Milunsky A (1992) An exonic mutation in the HuP2 paired domain gene causes Waardenburg's syndrome. Nature 355:637-8

7. Tassabehji M, Read AP, Newton VE, Harris R, Balling R, Gruss P, Strachan T (1992) Waardenburg's syndrome patients have mutations in the human homologue of the Pax-3 paired box gene. Nature 355:635-6

8. Tassabehji M, Newton VE, Read AP (1994) Waardenburg syndrome type 2 caused by mutations in the human microphthalmia (MITF) gene. Nat Genet 8:251-5

9. Sanchez-Martin M, Rodriguez-Garcia A, Perez-Losada J, Sagrera A, Read AP, Sanchez-Garcia I (2002) SLUG (SNAI2) deletions in patients with Waardenburg disease. Hum Mol Genet 11:3231-6

10. Shah KN, Dalal SJ, Desai MP, Sheth PN, Joshi NC, Ambani LM (1981) White forelock, pigmentary disorder of irides, and long segment Hirschsprung disease: possible variant of Waardenburg syndrome. J Pediatr 99:432-5

11. Puffenberger EG, Hosoda K, Washington SS, Nakao K, deWit D, Yanagisawa M, Chakravart A (1994) A missense mutation of the endothelin-B receptor gene in multigenic Hirschsprung's disease. Cell 79:1257-66

12. Chakravarti A (1996) Endothelin receptor-mediated signaling in hirschsprung disease. Hum Mol Genet 5:303-7

13. Edery P, Attie T, Amiel J, Pelet A, Eng C, Hofstra RM, Martelli H, Bidaud C, Munnich A, Lyonnet S (1996) Mutation of the endothelin-3 gene in the Waardenburg-Hirschsprung disease (Shah-Waardenburg syndrome). Nat Genet 12:442-4

14. Hofstra RM, Osinga J, Tan-Sindhunata G, Wu Y, Kamsteeg EJ, Stulp RP, van Ravenswaaij-Arts C, Majoor-Krakauer D, Angrist M, Chakravarti A, et al. (1996) A homozygous mutation in the endothelin-3 gene associated with a combined Waardenburg type 2 and Hirschsprung phenotype (Shah-Waardenburg syndrome). Nat Genet 12:445-7

15. McCallion AS, Chakravarti A (2001) EDNRB/EDN3 and Hirschsprung disease type II. Pigment Cell Res 14:161-9

16. Pingault V, Bondurand N, Lemort N, Sancandi M, Ceccherini I, Hugot JP, Jouk PS, Goossens M (2001) A heterozygous endothelin 3 mutation in Waardenburg-Hirschsprung disease: is there a dosage effect of EDN3/EDNRB gene mutations on neurocristopathy phenotypes? J Med Genet 38:205-9

17. Brooks AS, Oostra BA, Hofstra RM (2005) Studying the genetics of Hirschsprung's disease: unraveling an oligogenic disorder. Clin Genet 67:6-14

18. Pingault V, Bondurand N, Kuhlbrodt K, Goerich DE, Prehu MO, Puliti A, Herbarth B, Hermans-Borgmeyer I, Legius E, Matthijs G, et al. (1998) SOX10 mutations in patients with Waardenburg-Hirschsprung disease. Nat Genet 18:171-3

19. Kapur RP (1999) Early death of neural crest cells is responsible for total enteric aganglionosis in Sox10(Dom)/Sox10(Dom) mouse embryos. Pediatr Dev Pathol 2:559-69

20. Kim J, Lo L, Dormand E, Anderson DJ (2003) SOX10 maintains multipotency and inhibits neuronal differentiation of neural crest stem cells. Neuron 38:17-31

21. Wegner M (1999) From head to toes: the multiple facets of Sox proteins. Nucleic Acids Res 27:1409-20

22. Mollaaghababa R, Pavan WJ (2003) The importance of having your SOX on: role of SOX10 in the development of neural crest-derived melanocytes and glia. Oncogene 22:3024-34

23. Hong CS, Saint-Jeannet JP (2005) Sox proteins and neural crest development. Semin Cell Dev Biol 16:694-703

24. Wegner M, Stolt CC (2005) From stem cells to neurons and glia: a Soxist's view of neural development. Trends Neurosci 28:583-8

25. Kelsh RN (2006) Sorting out Sox10 functions in neural crest development. Bioessays 28:788-98

26. Foster JW, Dominguez-Steglich MA, Guioli S, Kowk G, Weller PA, Stevanovic M, Weissenbach J, Mansour S, Young ID, Goodfellow PN, et al. (1994) Campomelic dysplasia and autosomal sex reversal caused by mutations in an SRY-related gene. Nature 372:525-30

27. Wagner T, Wirth J, Meyer J, Zabel B, Held M, Zimmer J, Pasantes J, Bricarelli FD, Keutel J, Hustert E, et al. (1994) Autosomal sex reversal and campomelic dysplasia are caused by mutations in and around the SRY-related gene SOX9. Cell 79:1111-20

28. Bowles J, Schepers G, Koopman P (2000) Phylogeny of the SOX family of developmental transcription factors based on sequence and structural indicators. Dev Biol 227:239-55

29. Peirano RI, Goerich DE, Riethmacher D, Wegner M (2000) Protein zero gene expression is regulated by the glial transcription factor Sox10. Mol Cell Biol 20:3198-209

30. Bondurand N, Pingault V, Goerich DE, Lemort N, Sock E, Caignec CL, Wegner M, Goossens M (2000) Interaction among SOX10, PAX3 and MITF, three genes altered in Waardenburg syndrome. Hum Mol Genet 9:1907-17

31. Lang D, Chen F, Milewski R, Li J, Lu MM, Epstein JA (2000) Pax3 is required for enteric ganglia formation and functions with Sox10 to modulate expression of c-ret. J Clin Invest 106:963-71

32. Lee M, Goodall J, Verastegui C, Ballotti R, Goding CR (2000) Direct regulation of the Microphthalmia promoter by Sox10 links Waardenburg-Shah syndrome (WS4)-associated hypopigmentation and deafness to WS2. J Biol Chem 275:37978-83

33. Potterf SB, Furumura M, Dunn KJ, Arnheiter H, Pavan WJ (2000) Transcription factor hierarchy in Waardenburg syndrome: regulation of MITF expression by SOX10 and PAX3. Hum Genet 107:1-6

34. Verastegui C, Bille K, Ortonne JP, Ballotti R (2000) Regulation of the microphthalmia-associated transcription factor gene by the Waardenburg syndrome type 4 gene, SOX10. J Biol Chem 275:30757-60

35. Elworthy S, Lister JA, Carney TJ, Raible DW, Kelsh RN (2003) Transcriptional regulation of mitfa accounts for the sox10 requirement in zebrafish melanophore development. Development 130:2809-18

36. Jiao Z, Mollaaghababa R, Pavan WJ, Antonellis A, Green ED, Hornyak TJ (2004) Direct interaction of Sox10 with the promoter of murine Dopachrome Tautomerase (Dct) and synergistic activation of Dct expression with Mitf. Pigment Cell Res 17:352-62

37. Ludwig A, Rehberg S, Wegner M (2004) Melanocyte-specific expression of dopachrome tautomerase is dependent on synergistic gene activation by the Sox10 and Mitf transcription factors. FEBS Lett 556:236-44

38. Zhu L, Lee HO, Jordan CS, Cantrell VA, Southard-Smith EM, Shin MK (2004) Spatiotemporal regulation of endothelin receptor-B by SOX10 in neural crest-derived enteric neuron precursors. Nat Genet 36:732-7

39. Wegner M (2005) Secrets to a healthy Sox life: lessons for melanocytes. Pigment Cell Res 18:74-85

40. Yokoyama S, Takeda K, Shibahara S (2006) SOX10, in combination with Sp1, regulates the endothelin receptor type B gene in human melanocyte lineage cells. Febs J 273:1805-20

41. Murisier F, Guichard S, Beermann F (2007) The tyrosinase enhancer is activated by Sox10 and Mitf in mouse melanocytes. Pigment Cell Res 20:173-84

42. Peirano RI, Wegner M (2000) The glial transcription factor Sox10 binds to DNA both as monomer and dimer with different functional consequences. Nucleic Acids Res 28:3047-55

43. Bondurand N, Girard M, Pingault V, Lemort N, Dubourg O, Goossens M (2001) Human Connexin 32, a gap junction protein altered in the X-linked form of Charcot-Marie-Tooth disease, is directly regulated by the transcription factor SOX10. Hum Mol Genet 10:2783-95

44. Britsch S, Goerich DE, Riethmacher D, Peirano RI, Rossner M, Nave KA, Birchmeier C, Wegner M (2001) The transcription factor Sox10 is a key regulator of peripheral glial development. Genes Dev 15:66-78

45. Schlierf B, Ludwig A, Klenovsek K, Wegner M (2002) Cooperative binding of Sox10 to DNA: requirements and consequences. Nucleic Acids Res 30:5509-16

46. Stolt CC, Rehberg S, Ader M, Lommes P, Riethmacher D, Schachner M, Bartsch U, Wegner M (2002) Terminal differentiation of myelin-forming oligodendrocytes depends on the transcription factor Sox10. Genes Dev 16:165-70

47. Touraine RL, Attie-Bitach T, Pelet A, Auge J, Pingault V, Amiel J, Goossens M, Delezoide AL, Razavi F, Munnich A, et al. (1998) Expression of SOX10 in human embryo and fetal brain accounts for a neurological phenotype in Waardenburg type 4 spectrum. Am J Hum Genet 63:A174

48. Bondurand N, Kuhlbrodt K, Pingault V, Enderich J, Sajus M, Tommerup N, Warburg M, Hennekam RC, Read AP, Wegner M, et al. (1999) A molecular analysis of the yemenite deaf-blind hypopigmentation syndrome: SOX10 dysfunction causes different neurocristopathies. Hum Mol Genet 8:1785-9

49. Inoue K, Tanabe Y, Lupski JR (1999) Myelin deficiencies in both the central and the peripheral nervous systems associated with a SOX10 mutation. Ann Neurol 46:313-8

50. Southard-Smith EM, Angrist M, Ellison JS, Agarwala R, Baxevanis AD, Chakravarti A, Pavan WJ (1999) The Sox10(Dom) mouse: modeling the genetic variation of Waardenburg-Shah (WS4) syndrome. Genome Res 9:215-25

51. Pingault V, Guiochon-Mantel A, Bondurand N, Faure C, Lacroix C, Lyonnet S, Goossens M, Landrieu P (2000) Peripheral neuropathy with hypomyelination, chronic intestinal pseudo-obstruction and deafness: a developmental "neural crest syndrome" related to a SOX10 mutation. Ann Neurol 48:671-6

52. Touraine RL, Attie-Bitach T, Manceau E, Korsch E, Sarda P, Pingault V, Encha-Razavi F, Pelet A, Auge J, Nivelon-Chevallier A, et al. (2000) Neurological phenotype in Waardenburg syndrome type 4 correlates with novel SOX10 truncating mutations and expression in developing brain. Am J Hum Genet 66:1496-503

53. Sham MH, Lui VC, Chen BL, Fu M, Tam PK (2001) Novel mutations of SOX10 suggest a dominant negative role in Waardenburg-Shah syndrome. J Med Genet 38:E30

54. Inoue K, Shilo K, Boerkoel CF, Crowe C, Sawady J, Lupski JR, Agamanolis DP (2002) Congenital hypomyelinating neuropathy, central dysmyelination, and Waardenburg-Hirschsprung disease: phenotypes linked by SOX10 mutation. Ann Neurol 52:836-42

55. Pingault V, Girard M, Bondurand N, Dorkins H, Van Maldergem L, Mowat D, Shimotake T, Verma I, Baumann C, Goossens M (2002) SOX10 mutations in chronic intestinal pseudo-obstruction suggest a complex physiopathological mechanism. Hum Genet 111:198-206

56. Toki F, Suzuki N, Inoue K, Suzuki M, Hirakata K, Nagai K, Kuroiwa M, Lupski JR, Tsuchida Y (2003) Intestinal aganglionosis associated with the Waardenburg syndrome: report of two cases and review of the literature. Pediatr Surg Int 19:725-8

57. Inoue K, Khajavi M, Ohyama T, Hirabayashi S, Wilson J, Reggin JD, Mancias P, Butler IJ, Wilkinson MF, Wegner M, et al. (2004) Molecular mechanism for distinct neurological phenotypes conveyed by allelic truncating mutations. Nat Genet 36:361-9

58. Verheij JB, Sival DA, van der Hoeven JH, Vos YJ, Meiners LC, Brouwer OF, van Essen AJ (2006) Shah-Waardenburg syndrome and PCWH associated with SOX10 mutations: a case report and review of the literature. Eur J Paediatr Neurol 10:11-7

59. Niel F, Martin J, Dastot-Le Moal F, Costes B, Boissier B, Delattre V, Goossens M, Girodon E (2004) Rapid detection of CFTR gene rearrangements impacts on genetic counselling in cystic fibrosis. J Med Genet 41:e118

60. Dastot-Le Moal F, Wilson M, Mowat D, Collot N, Niel F, Goossens M (2007) ZFHX1B mutations in patients with Mowat-Wilson syndrome. Hum Mutat 28:313-21

61. Yau SC, Bobrow M, Mathew CG, Abbs SJ (1996) Accurate diagnosis of carriers of deletions and duplications in Duchenne/Becker muscular dystrophy by fluorescent dosage analysis. J Med Genet 33:550-8

62. Pinkel D, Straume T, Gray JW (1986) Cytogenetic analysis using quantitative, high-sensitivity, fluorescence hybridization. Proc Natl Acad Sci U S A 83:2934-8

63. Girard M, Goossens M (2006) Sumoylation of the SOX10 transcription factor regulates its transcriptional activity. FEBS Lett 580:1635-41

64. Maka M, Stolt CC, Wegner M (2005) Identification of Sox8 as a modifier gene in a mouse model of Hirschsprung disease reveals underlying molecular defect. Dev Biol 277:155-69

65. Antonellis A, Bennett WR, Menheniott TR, Prasad AB, Lee-Lin SQ, Green ED, Paisley D, Kelsh RN, Pavan WJ, Ward A (2006) Deletion of long-range sequences at Sox10 compromises developmental expression in a mouse model of Waardenburg-Shah (WS4) syndrome. Hum Mol Genet 15:259-71

66. Sock E, Pagon RA, Keymolen K, Lissens W, Wegner M, Scherer G (2003) Loss of DNA-dependent dimerization of the transcription factor SOX9 as a cause for campomelic dysplasia. Hum Mol Genet 12:1439-47

67. Houlden H, Girard M, Cockerell C, Ingram D, Wood NW, Goossens M, Walker RW, Reilly MM (2004) Connexin 32 promoter P2 mutations: a mechanism of peripheral nerve dysfunction. Ann Neurol 56:730-4

68. Lang D, Epstein JA (2003) Sox10 and Pax3 physically interact to mediate activation of a conserved c-RET enhancer. Hum Mol Genet 12:937-45

69. Morgan NV, Westaway SK, Morton JE, Gregory A, Gissen P, Sonek S, Cangul H, Coryell J, Canham N, Nardocci N, et al. (2006) PLA2G6, encoding a phospholipase A2, is mutated in neurodegenerative disorders with high brain iron. Nat Genet 38:752-4

70. Shahin H, Walsh T, Sobe T, Abu Sa'ed J, Abu Rayan A, Lynch ED, Lee MK, Avraham KB, King MC, Kanaan M (2006) Mutations in a novel isoform of TRIOBP that encodes a filamentous-actin binding protein are responsible for DFNB28 recessive nonsyndromic hearing loss. Am J Hum Genet 78:144-52

71. Lalwani AK, Goldstein JA, Kelley MJ, Luxford W, Castelein CM, Mhatre AN (2000) Human nonsyndromic hereditary deafness DFNA17 is due to a mutation in nonmuscle myosin MYH9. Am J Hum Genet 67:1121-8

72. Heath KE, Campos-Barros A, Toren A, Rozenfeld-Granot G, Carlsson LE, Savige J, Denison JC, Gregory MC, White JG, Barker DF, et al. (2001) Nonmuscle myosin heavy chain IIA mutations define a spectrum of autosomal dominant macrothrombocytopenias: May-Hegglin anomaly and Fechtner, Sebastian, Epstein, and Alport-like syndromes. Am J Hum Genet 69:1033-45

73. Phelan MC, Rogers RC, Saul RA, Stapleton GA, Sweet K, McDermid H, Shaw SR, Claytor J, Willis J, Kelly DP (2001) 22q13 deletion syndrome. Am J Med Genet 101:91-9

74. Bonaglia MC, Giorda R, Mani E, Aceti G, Anderlid BM, Baroncini A, Pramparo T, Zuffardi O (2006) Identification of a recurrent breakpoint within the SHANK3 gene in the 22q13.3 deletion syndrome. J Med Genet 43:822-8

75. Attie T, Pelet A, Edery P, Eng C, Mulligan LM, Amiel J, Boutrand L, Beldjord C, Nihoul-Fekete C, Munnich A, et al. (1995) Diversity of RET proto-oncogene mutations in familial and sporadic Hirschsprung disease. Hum Mol Genet 4:1381-6

76. de Pontual L, Pelet A, Clement-Ziza M, Trochet D, Antonarakis SE, Attie-Bitach T, Beales PL, Blouin JL, Dastot-Le Moal F, Dollfus H, et al. (2007) Epistatic interactions with a common hypomorphic RET allele in syndromic Hirschsprung disease. Hum Mutat 28:790-796

77. Wong WT, Agron E, Coleman HR, Reed GF, Csaky K, Peterson J, Glenn G, Linehan WM, Albert P, Chew EY (2007) Genotype-phenotype correlation in von Hippel-Lindau disease with retinal angiomatosis. Arch Ophthalmol 125:239-45

78. Kellerer S, Schreiner S, Stolt CC, Scholz S, Bosl MR, Wegner M (2006) Replacement of the Sox10 transcription factor by Sox8 reveals incomplete functional equivalence. Development 133:2875-86

Table 1

Primer	Primer sequence (5'→3') Forward	Reverse	reaction mix	PCR size	Gene-position NC
Reference genes					
DSCR1	GCGACGAGGACGCATTCCAA	GTCCTTGTGCGATCACCACA	1 and 2	238	*DSCR1*-exon4 NC_000021.7
F9	AAATGATGCTGTTACTGTCTA	GAAGTTTCAGATACAGATTTTC	1 and 2	214	*F*9-exon5 NC_000023.9
***SOX10* gene**					
P5	GGCCAGGCGAGCTGGGCAAGGTC	GAATCCACCCGAAGCTAGAG	1	341	*SOX10*-Exon3 NC_000022.9
P6	GGAGTGCTCTGGCATTCACG	CTTGCCCCACCCTCAGCTCT	1	366	*SOX10*-Exon4 NC_000022.9
P7	GGAAGTTCACGTGCGCCCAC	GCGGCAGGTACTGGTCCAAC	1	286	*SOX10*-Exon5 NC_000022.9
P8	CCACACTACACCGACCAGCC	GGGTGGTGGCGACAGGGC	1	326	*SOX10*-Exon5 NC_000022.9
External markers					
P9	GATGACGTTTCTAGGTGG	TGTTCCTAAGGATCTGTAGG	1	309	*POLR2F*-exon4 NC_000022.9
P1	GAGGAGGGAGTTTGGGTGGGTGG	GCACAGGATGGGACGGGTTGAGA	2	310	-54694/-55003 NC000022.9
P2	TGGGAACAATGTCAACGTCG	CAGAAGGCCTCCTCCAATGA	2	330	-32490/-32819 NC000022.9
P3	TACCAGGGCGGGCTCCTGTA	GCCCCTGTTCCTTCCAGACTCCC	2	363	-14793/-15155 NC000022.9
P4	ACACGACGGCAGATGCTCGT	CCTCGGAGCCCAGTGAATTA	2	335	-2116/-2450 NC000022.9

Table 1. Multiplex QMF-PCR primer sequences. GenBank, accession number (NC), position, sequences, expected PCR product size (bp) of primers P1 to P9. Position of primers P1 to P4 are indicated with the A of the *SOX10* ATG numbered as 1. Homo sapiens Build 36.2 was used.

Table 2

	5' *SOX10* region	***SOX10* gene**				***POLR2F* gene**
	S4 (P4)	**exon 3 (P5)**	**exon 4 (P6)**	**exon 5 (P7)**	**exon 5 (P8)**	**exon 4 (P9)**
Subject 1	1.07	1.02	1.12	1.02	1.02	1.00
Subject 2	1.02	1.08	1.03	0.97	0.93	0.94
Patient 1	1.00	1.02	0.96	**0.47**	1.10	0.86
Patient 2	**0.46**	**0.50**	**0.46**	**0.51**	**0.49**	**0.45**
Patient 3	**0.47**	**0.47**	**0.48**	**0.51**	**0.51**	**0.51**
Patient 4	1.20	**0.58**	0.90	1.17	1.20	0.83
Patient 5	0.90	1.10	**0.56**	1.08	0.96	0.99
Patient 6	**0.52**	**0.54**	**0.48**	**0.52**	**0.56**	**0.43**
Patient 7	**0.56**	**0.56**	**0.45**	**0.54**	**0.57**	**0.48**
Patient 8	**0.51**	**0.46**	**0.53**	**0.50**	**0.49**	**0.50**

Table 2. DQ values from QMF-PCR performed with mix 1. The analysis is based on the comparison of the peak height from the tested DNA (two non deleted patients called subject 1-2 and patients 1 to 8) and control DNA samples. The copy-number change for each amplicon was calculated using the peak value normalised to the peak value of the *DSCR1* gene exon 4.

Table 3

Primer sequence (5'→3')		
Forward	**Reverse**	**Gene-position and NC**
CGCCTCAGCTACCCCTCAGC	CCGGCCCCAGCGTACCTGTA	*FBX07*-exon1 NC_000022.9
CTGGAGGGGTAGCAGTTAGC	GATCGTTCAGATCCTTATAG	*TIMP3*-exon1 NC_000022.9
GATCAACAACTGTCAGCTCC	CCTGCAGGTGGAGGCTGAGG	*ISX*-exon1 NC_000022.9
CGGTAGCAGCAATGGACTTT	TCCTTACCTACTGGCTGTCA	*TOM1*-exon1 NC_000022.9
TTCAGGCATCTTCCTTGCAC	AAGTCACTAACACTCAGCTC	*APOL3*-exon4 NC_000022.9
AGGCGGCTGTCTCCACCGGG	GAGTGATTGTCTCAAAAGGC	*MYH9*-intron1 NC_000022.9
CACACTCTCCCGAGAACCAG	CAAGTACCTTCTAGGCAGCA	*CACNG2*-exon1 NC_000022.9
GAGAGCCTGGCCTGGACACA	GAAAGAGGACATGTTGAACC	*LGALS2*-exon4 NC_000022.9
TGTGACGGATGATTTCAGAT	ATGCCCTCAGAAAGCAGCAT	*SH3BP1*-exon10 NC_000022.9
GGTGAAATTCCTCAGCTCTC	GTATCTTACTTGTGCAAGGG	*TRIOBP*-exon1 NC_000022.9
CCCATGGATCACGCTGGTGC	TAGGGGTGATGCCGTACCAG	*MICALL1*-exon8 NC_000022.9
TATAATGTACATGCTGCTGT	GTACTGAGCCCAGGCAATCC	*MICALL1*-intron9 NC_000022.9
GACATCCATGGAGAGATGGA	GAGCTCGGACTCTCGCCGCA	*MICALL1*-exon11-12 NC_000022.9
GGCAGCGGTGATTCAGCCCT	ACTGAGATCCAAGGGCGCCT	*MICALL1*-exon16 NC_000022.9
GATGCTTTGCCCCTACAGTG	GCTGAGGCTCAAGAGCATTG	*C22ORF23*-exon4 NC_000022.9
CAGAGGGCAGAAATTTTATT	CATGATGTCCATGATGTGGC	*C22ORF23*-exon3 NC_000022.9
CAGTCAGCGCATGCGCACTT	CAGACATTGCCCCTAGACGC	*POLR2F*-exon1 NC_000022.9
CAGAGGTAATCAAGTTAGCC	GTATTAGGATGGGTCGTAGG	P2_3-4 -20540/-20829 NC_000022.9
CACCTGGCCAGGATGAGCTT	CCACAGTGAGCACTCAGGAA	P2_3-3 -21390/-21739 NC_000022.9
TTGTAAAGCAACAGAGGAGC	CCTTCCGCAAAGACTTGCTG	P2_3-2 -23920/-24166 NC_000022.9
CCAAAAGCAGAAATCTGGGA	GGCCTGAGGCTCCAGCTGAG	P2_3-1 -31482/-31759 NC_000022.9
GATGGGATGGGAGGCAGTCT	CCGTGGGTCAGCAGCACTAT	*PLA2G6*-exon7 NC_000022.9
GGCGGGAATGCTCTTGAGCT	CACCCTGGACAGCATAATGG	*PLA2G6*-exon4 NC_000022.9
GGCTTCAGGAGGGCAGAGCA	CCAGGGCTTTTAACATACCA	*PLA2G6*-intron2 NC_000022.9
CCTTCAGTGGCGTCACCAAC	GGTCCAAGAGTACAGTCTCC	*PLA2G6*-exon2 NC_000022.9
CTCTAGACCTGGGGCCTCCG	ATGCAGGCCTCTGCCACGAG	*C22ORF5*-exon9 NC_000022.9
TGGACCATGAACGTGTTCCG	ATCATCTCGAGGGGTCCTCC	*KDELR3*-exon1 NC_000022.9
TTGTGCAGTCGCTGGGAAGG	GATAGAGATCTGGGAGCGGG	*DDX17*-exon1 NC_000022.9
TCCTACCCCATCTGCCTTCT	CCTGGAGCCTCCCAAAGGGC	*CBX7*-intron1 NC_000022.9
AGCCTGTGGCTTGGAGTGGC	GTGGGAGCTCAGATCCCACC	*PDGFB*-exon7 NC_000022.9

Table 3. Additional QMF-PCR primers, ordered centromeric to telomeric. Position of primers P2_3-1 to 4 located between P2 and P3 (see table1) are given with the A of the SOX10 ATG numbered as 1. Homo sapiens Build 36.2 was used. NC: accession number

Table 4

Patient				Phenotype					Molecular defect		
N°	**Gender**	**Age**	**WS type**	**Deafness**	**Pig.Ano.**	**HSCR**	**M R**	**Others**	**Inheritance**	**Del. nomenclature**	**Del. size**
1	M	1y	WS4	Bilateral	Hair and skin	Short	No	Bilateral cryptorchidism	De novo	c.697-740_1085delinsCCT	1128pb + ins3bp
2	M	13y	PCWH	Profound bilateral	Hair and skin, sapphire blue eyes	Short	Mild	Anosmia, hypermetropia, dental enamal abnormalities	De novo	g.(17,738,296_17,740,110)_(17,794,727_17,801,789) del (NCBI Build 36.2)	56 to 68 kb
3	M	36y	PCWH	Profound bilateral	Hair and skin, sapphire blue eyes	Short	Mild	Anosmia, cryptorchidism hypogonadism	De novo	g.(17,712,505_17,716,229)_(17,929,647_17,933,832) del (NCBI Build 36.2)	213 to 222 kb
4& B	M	9y	WS2	Profound bilateral	Skin, irides and retinal hypo-pig.	No	No		Maternal (mosaicism)	c.219_428+43del	253 bp
5	M	8y	WS2	Profound bilateral	Skin, hypoplastic irides	No	No		Maternal	c.429-1112_697+396del	1777 bp
6	M	8y	WS2	Profound bilateral	White frontal forelock, heterochromia irides	No	No		De novo	g.(16,173,196_16,489,188)_(17,790,847_17,791,697) del (NCBI Build 36.2)	1.3 to 1.6 Mb
7	M	23y	WS2	Bilateral	Skin, saphire blue eyes	No	Severe	Short stature, pectus excavatum, autism	De novo	g.(17,357,039_17,432,022)_(18,006,412_18,254,748) del (NCBI Build 36.2)	574 to 898 kp
8	F	19m	WS2	Yes	Skin, white forelock	No	Delayed	Thumb duplication, congenital heart disease	De novo	g.(Z83846_Z69042)_(18,938,054_19,010,379)del (NCBI Build 36.2)	5.5 to 6.1 Mb

Table 4. Summary of clinical findings. The deletions are described in relation to the human genome reference sequence NCBI Built36.2 NT_011520.11. N°: number;B: brother; y: years; m:months; Pig.Ano: pigmentation anomalies; hypo-pig: hypopigmentation; MR: mental retardation; Del.: deletion.

Figure legends:

Figure 1: ***SOX10* deletions in patients presenting with classical form of WS4 or PCWH.** (A) Schematic representation of the 3 deletions identified by QMF-PCR. Scheme on the top indicates the *SOX10* gene structure (an approximate scale is shown on the right). *SOX10* coding sequence (exons 3 to 5) is indicated with black boxes, and non coding exonic sequence with white boxes. Arrowheads indicate the position of the segments analysed by multiplex QMF-PCR (P1 to P9; see table 1 for corresponding primers sequences). They include the downstream adjacent *POLR2F* gene (grey box) and 4 short regions located up to 50kb upstream of *SOX10*, indicated by dark lines and called S1 to S4. QMF-PCR results of patients 1 to 3 are indicated below: '+' = not deleted or '-' = deleted. The phenotypes are indicated on the left. (B) Schematic representation (top) and electropherogram (bottom) of the deletion breakpoint region of patient 1. The size of the deletion and the nucleotidic localisation of the breakpoint are indicated on the diagram. The 3 inserted nucleotides are boxed. (C) Hybridization pattern of patients 2 and 3 using the BAC clone RP5-1039K5 encompassing the *SOX10* locus (indicated on the top of scheme A). The BAC clone RP5-1039K5 is labelled in red and the control probe in green (RP1-41P2). The normal chromosome 22 is indicated by an arrow and the deleted chromosome 22 by an arrowhead.

Figure 2: Functional consequences of the p.Val92Leu (V92L) mutation. (A) Amino acid sequence comparison of the region immediately preceding the HMG domain of SOX10 proteins across evolution and of SOX subgroup E proteins (human sequences). Gaps are indicated by blanks. The first part of HMG domain is boxed, and the amino acid substitution V92L from patient 3 is indicated by an arrow. *SOX10* sequence references: human (accession number NP_008872.1); mouse (XP_128139.4); chicken (NP_990123.1); fugu (NP_001072112.1); zebrafish (NP_571950.1); human SOX8 (NP_055402.2) and human SOX9 (NP_000337.1). (B) Subcellular localization of wild-type SOX10 and p.Val92Leu

mutant: HeLa cells were transfected with pECE-SOX10 (WT) or mutant (V92L) constructs for 24h, fixed and immunostained for SOX10. Cultures were counterstained with Dapi. (C and D) Transactivation capacities of SOX10 proteins. The *MITF* promoter (pMITF) (C) or the *GJB1* (pCx32) (D) promoter luciferase reporters were transfected in Hela cells in combination with wild type (WT) or mutant SOX10 proteins (V92L; E189X; 482ins6; Y313X), and /or PAX3 (C) or EGR2 (D). Reporter gene activations are presented as fold induction relative to the empty expression vector (pECE). Results represent the mean ± SME from 6 experiments, each performed in duplicate. Insets in C, D show a schematic representation of relative localisation of SOX10 (white boxes), PAX3 (striped circles) or EGR2 (striped triangle) binding sites on *MITF* or *GJB1* (Cx32) promoters.

Figure 3: Determination of the extent of large deletions in PCWH patients. Schematic representation of the deletions in patients 2 and 3, determined by FISH (A) or QMF-PCR experiments (B). Representative FISH results are shown in (A). The names of the BACs used for hybridization are indicated on each panel. Scheme (B) indicates the names, positions and orientation of genes located proximal or distal of *SOX10*. An approximate scale is shown. BACs used for FISH experiments are shown on the left and segments analysed by multiplex QMF-PCR are indicated by arrowheads (see table 3 for corresponding primers sequences). QMF-PCR results of patients 2 and 3 are indicated next to the corresponding fragments: '+' = not deleted or '-' = deleted.

Figure 4: ***SOX10* deletions in patients presenting with WS2**. (A) Schematic representation of the 5 deletions identified by QMF-PCR. Scheme on the top indicates the *SOX10* gene structure, QMF-PCR experiments results ('+' = non deleted or '-' = deleted) as described in Figure 1. (B and D) Schematic representation (top) and electropherograms (bottom) of the breakpoint deletion region of patient 4 (B) and patient 5 (D) and their relatives. The size of the deletions and the breakpoints are indicated on the scheme. (C) PCR covering exons 3 and

intron-exons boundaries using patient 4, his brother, mother and father's DNAs extracted from leucocytes (L), buccal cells (B), uroepithelial cells (U) and hair roots (H). The normal band is indicated by an arrow and the mutant allele by an arrowhead. Note the faint mutant band in the mother's uroepithelial cells. (E) Representative FISH result obtained for patient 8 with the probe RP5-1039K5 encompassing the *SOX10* locus (indicated on the top of scheme A). The BAC clone RP5-1039K5 is labelled in red and the control probe (RP1-127L4) in green. The normal chromosome 22 is indicated by an arrow and the deleted chromosome 22 by an arrowhead.

Figure 5: Determination of the extent of large deletions in WS2. Schematic representation of the deletions in patients 6, 7 and 8, determined by FISH (A) or QMF-PCR experiments (B) as described in figure 3. Only the first not deleted or partially deleted BACs are shown in (A).

Figure 1

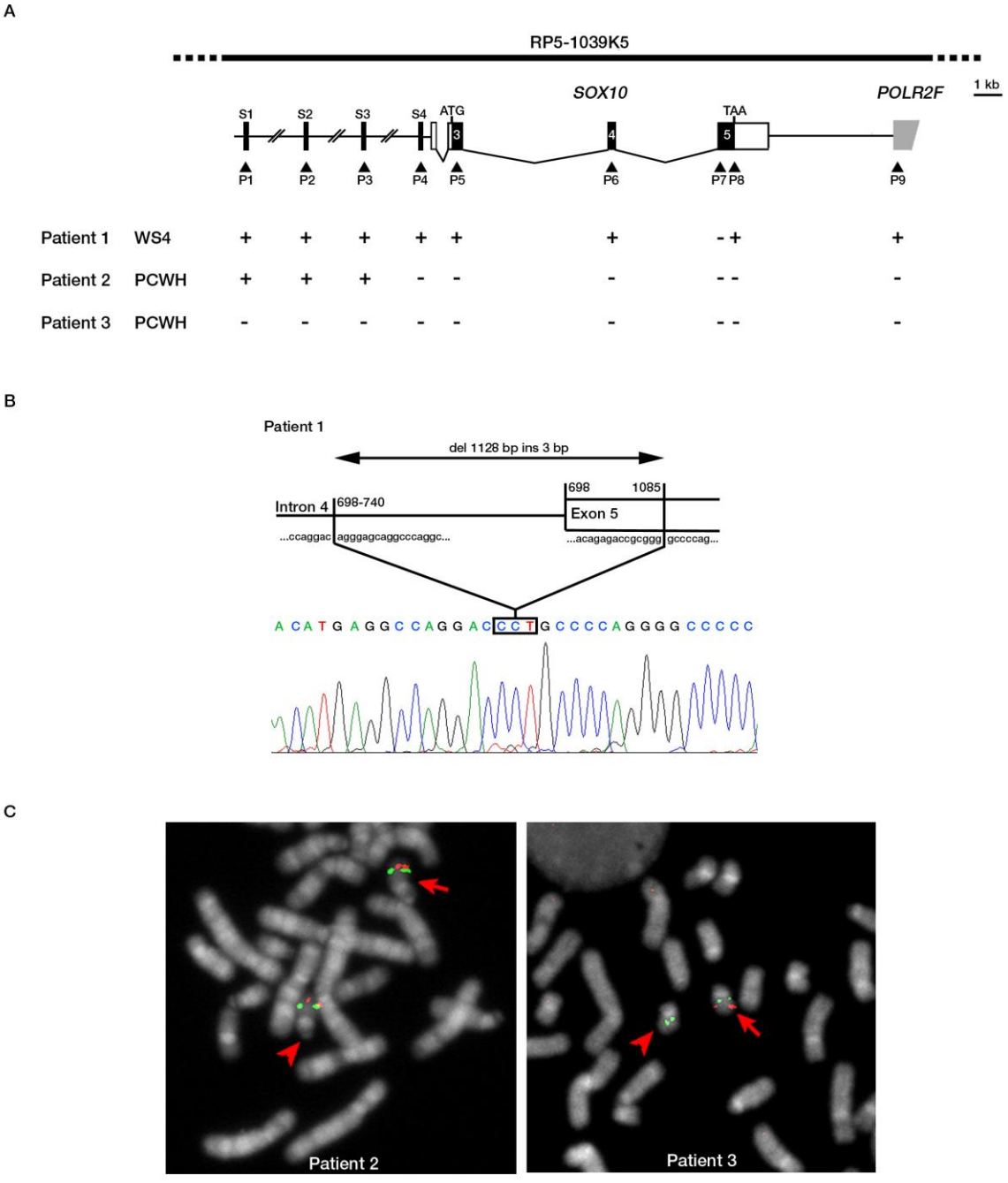
A
RP5-1039K5
SOX10
POLR2F
1 kb
S1
S2
S3
S4
ATG
TAA
P1
P2
P3
P4
P5
P6
P7 P8
P9
Patient 1 WS4 + + + + + + - + +
Patient 2 PCWH + + + - - - - - -
Patient 3 PCWH - - - - - - - - -
B
Patient 1
del 1128 bp ins 3 bp
Intron 4
698-740
698
1085
Exon 5
...ccaggac agggagcaggcccaggc...
...acagagaccgcggg gccccag...
A C A T G A G G C C A G G A C C C T G C C C C A G G G G C C C C C
C
Patient 2
Patient 3

Figure 2

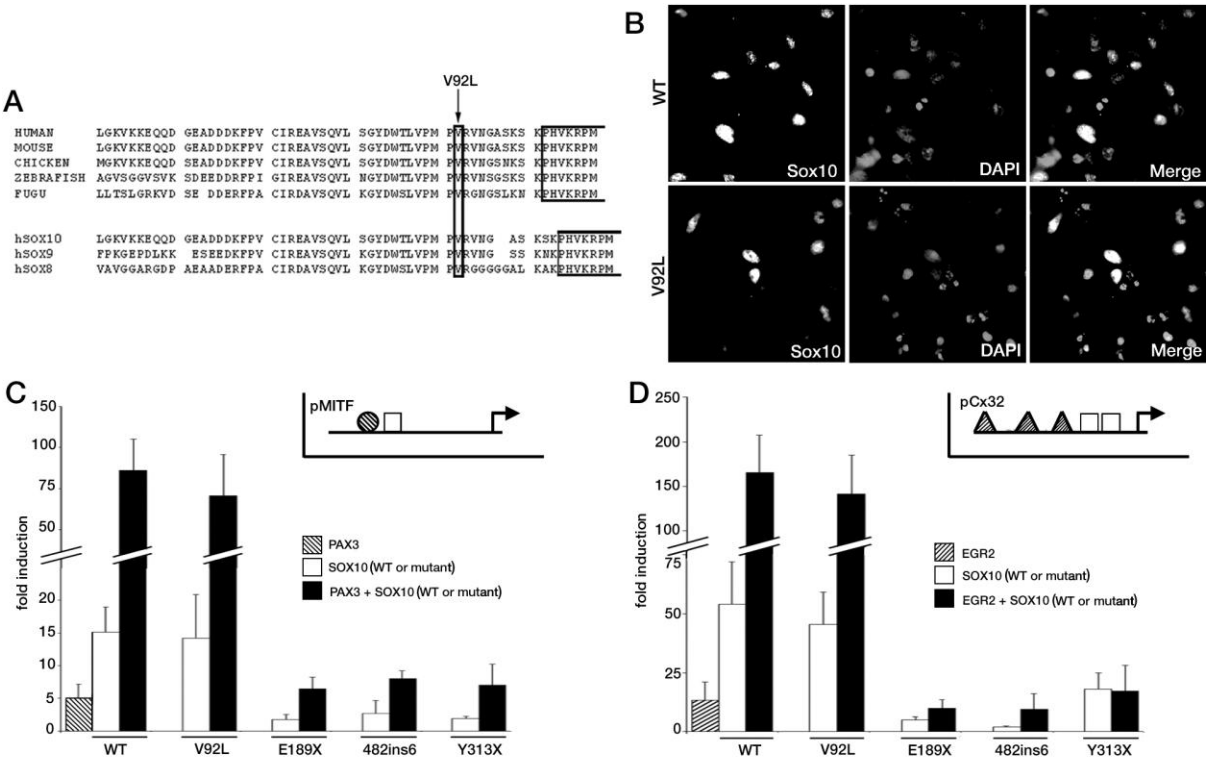
A
V92L
HUMAN LGKVKKEQQD GEADDDKFPV CIREAVSQVL SGYDWTLVPM PVRVNGASKS KPHVKRPM
MOUSE LGKVKKEQQD GEADDDKFPV CIREAVSQVL SGYDWTLVPM PVRVNGASKS KPHVKRPM
CHICKEN MGKVKKEQQD SEADDDKFPV CIREAVSQVL SGYDWTLVPM PVRVNGSNKS KPHVKRPM
ZEBRAFISH AGVSGGVSVK SDEEDDRFPI GIREAVSQVL NGYDWTLVPM PVRVNSGSKS KPHVKRPM
FUGU LLTSLGRKVD SE DDERFPA CIRDAVSQVL KGYDWSLVPM PVRGNGSLKN KPHVKRPM
hSOX10 LGKVKKEQQD GEADDDKFPV CIREAVSQVL SGYDWTLVPM PVRVNG AS KSKPHVKRPM
hSOX9 FPKGEPDLKK ESEEDKFPV CIREAVSQVL KGYDWTLVPM PVRVNG SS KNKPHVKRPM
hSOX8 VAVGGARGDP AEAADERFPA CIRDAVSQVL KGYDWSLVPM PVRGGGGGAL KAKPHVKRPM
B
WT
V92L
Sox10
DAPI
Merge
C
pMITF
fold induction
PAX3
SOX10 (WT or mutant)
PAX3 + SOX10 (WT or mutant)
WT
V92L
E189X
482ins6
Y313X
D
pCx32
fold induction
EGR2
SOX10 (WT or mutant)
EGR2 + SOX10 (WT or mutant)
WT
V92L
E189X
482ins6
Y313X

Figure 3

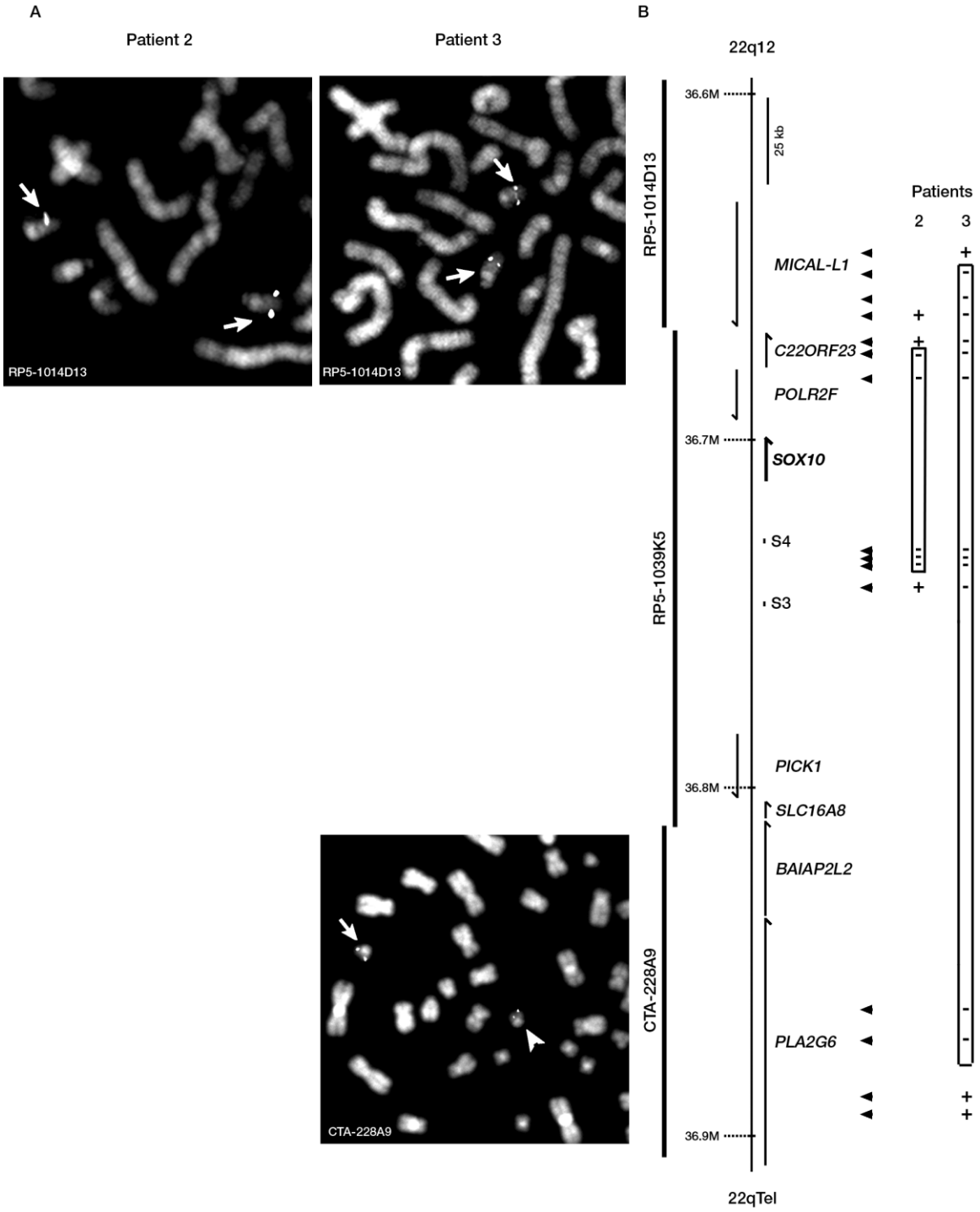
A
Patient 2
Patient 3
RP5-1014D13
RP5-1014D13
CTA-228A9
B
22q12
36.6M
25 kb
RP5-1014D13
MICAL-L1
C22ORF23
POLR2F
36.7M
SOX10
S4
S3
RP5-1039K5
PICK1
36.8M
SLC16A8
BAIAP2L2
CTA-228A9
PLA2G6
36.9M
22qTel
Patients
2
3

Figure 4

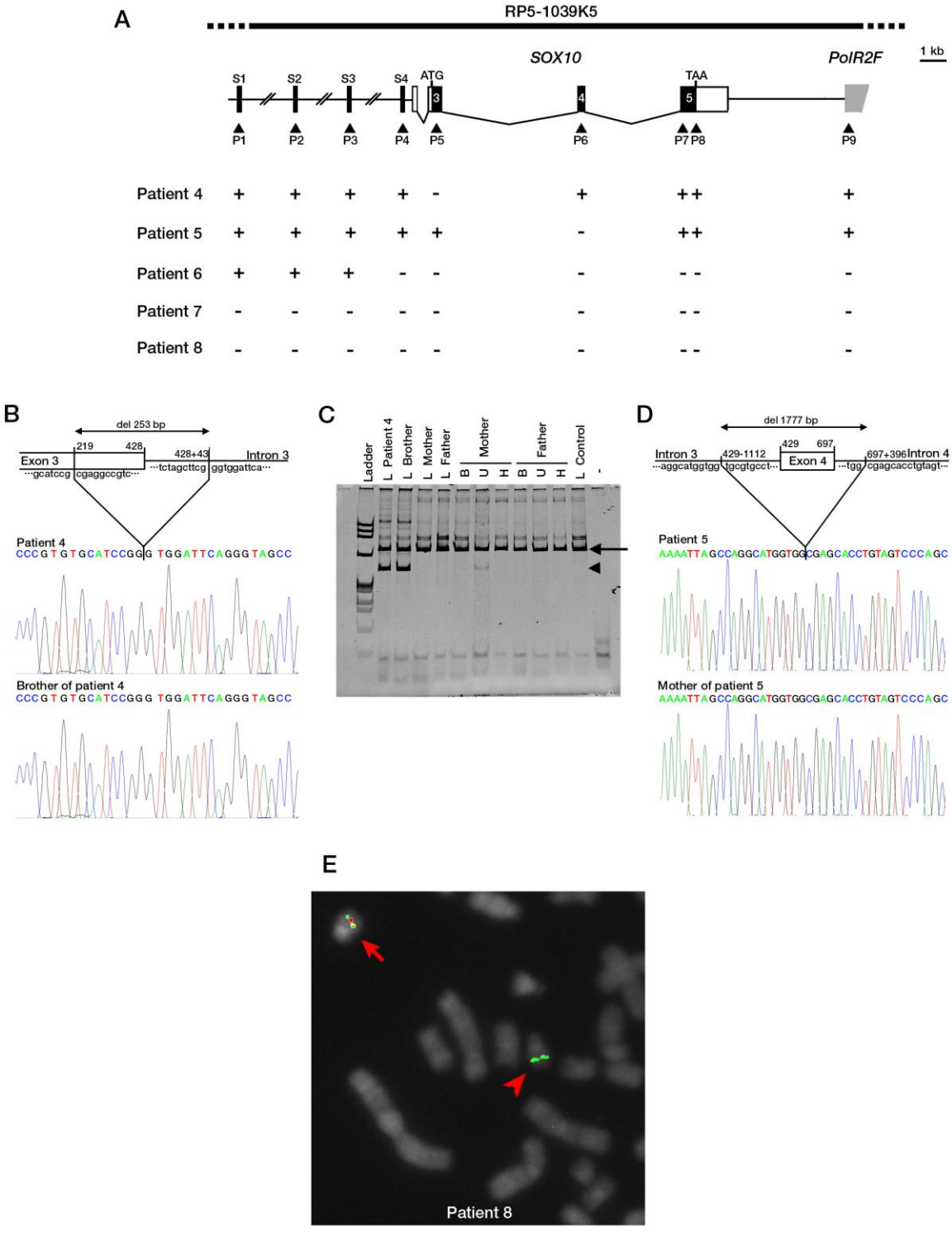
A
RP5-1039K5
SOX10
PolR2F
1 kb
S1 S2 S3 S4 ATG TAA
P1 P2 P3 P4 P5 P6 P7 P8 P9
Patient 4 + + + + - + ++ +
Patient 5 + + + + + - ++ +
Patient 6 + + + - - - - - -
Patient 7 - - - - - - - - -
Patient 8 - - - - - - - - -
B
del 253 bp
Exon 3
219
428
428+43
Intron 3
···gcatccg cgaggccgtc··· ···tctagcttcg ggtggattca···
Patient 4
CCCGTGTGCATCCGGG TGGATTTCAGGGTAGCC
Brother of patient 4
CCCGTGTGCATCCGGG TGGATTTCAGGGTAGCC
C
Ladder
L Patient 4
L Brother
L Mother
L Father
B U H Mother
B U H Father
L Control
-
D
del 1777 bp
Intron 3
429-1112
429
697
697+396Intron 4
Exon 4
···aggcatggtgg tgcgtgcct··· ···tgg cgagcacctgtagt···
Patient 5
AAAATTAGCCAGGCATGGTGGCGAGCACCTGTAGTCCCAGC
Mother of patient 5
AAAATTAGCCAGGCATGGTGGCGAGCACCTGTAGTCCCAGC
E
Patient 8

Figure 5

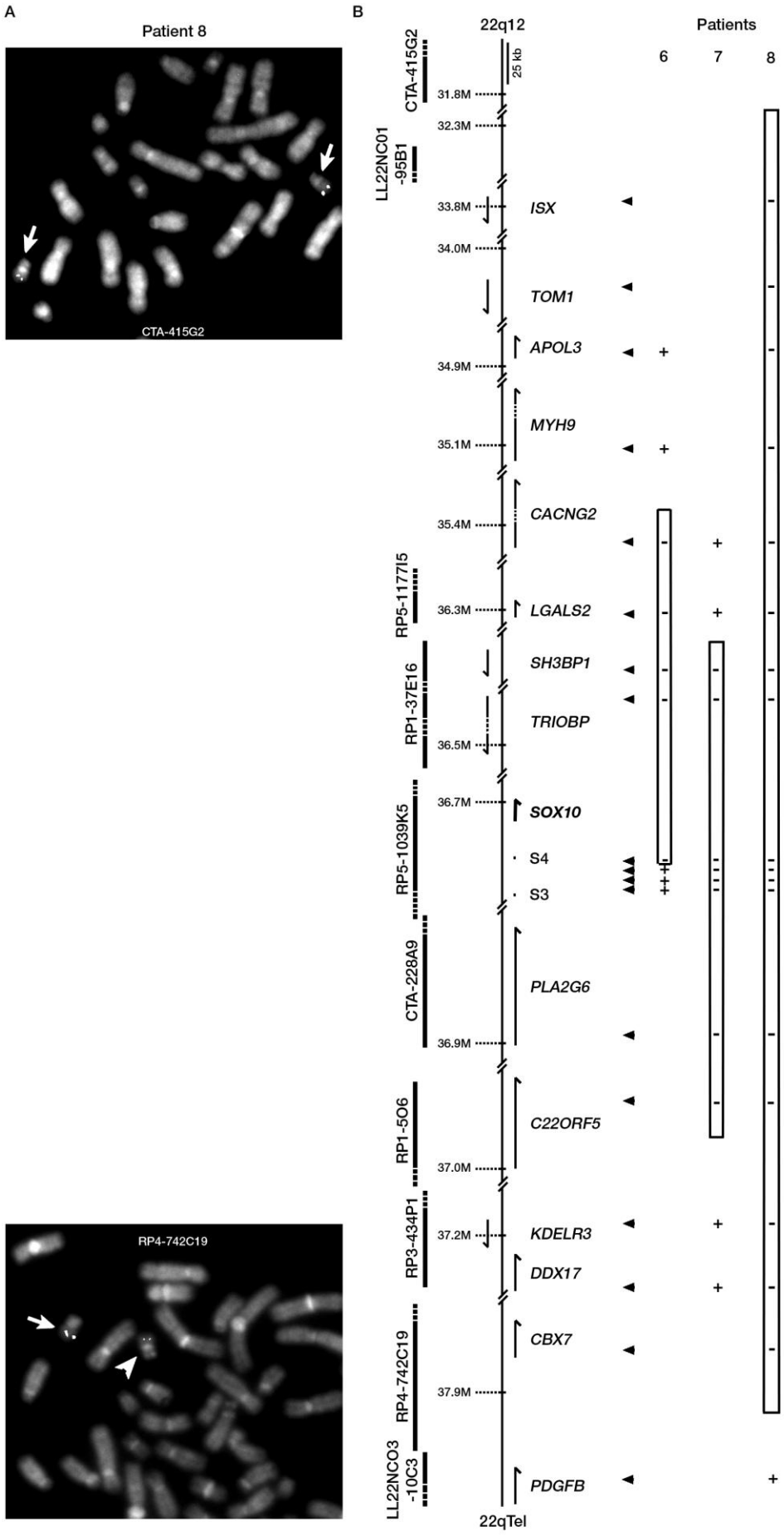
A
Patient 8
CTA-415G2
RP4-742C19
B
22q12
Patients
6
7
8
25 kb
CTA-415G2
31.8M
32.3M
LL22NC01
-95B1
33.8M
ISX
34.0M
TOM1
APOL3
34.9M
MYH9
35.1M
CACNG2
35.4M
RP5-1177I5
36.3M
LGALS2
SH3BP1
RP1-37E16
TRIOBP
36.5M
36.7M
SOX10
RP5-1039K5
S4
S3
CTA-228A9
PLA2G6
36.9M
RP1-5O6
C22ORF5
37.0M
RP3-434P1
37.2M
KDELR3
DDX17
CBX7
RP4-742C19
37.9M
LL22NCO3
-10C3
PDGFB
22qTel